Cell Insight 2 (2023) 100126

Contents lists available at ScienceDirect

Cell Insight

journal homepage: www.journals.elsevier.com/cell-insight

Research Article

Characterization of a thermostable Cas12a ortholog

Jing Wu [a,b], Pan Gao [a,c], Yajing Shi [a,c], Caixiang Zhang [a,c], Xiaohan Tong [a,b], Huidi Fan [d], Xi Zhou [d], Ying Zhang [a,c], Hao Yin [a,b,e,f,*]

[a] Department of Clinical Laboratory, Frontier Science Center for Immunology and Metabolism, Medical Research Institute, Zhongnan Hospital of Wuhan University, Wuhan University, Wuhan, 430071, China
[b] State Key Laboratory of Virology, TaiKang Centre for Life and Medical Sciences, TaiKang Medical School, Wuhan University, Wuhan, 430071, China
[c] Department of Rheumatology and Immunology, Zhongnan Hospital of Wuhan University, Wuhan University, Wuhan, 430071, China
[d] State Key Laboratory of Virology, Wuhan Institute of Virology, Wuhan, 430071, China
[e] Wuhan Research Center for Infectious Diseases and Cancer, Chinese Academy of Medical Sciences, Wuhan, 430071, China
[f] Department of Urology, Frontier Science Center for Immunology and Metabolism, Medical Research Institute, Zhongnan Hospital of Wuhan University, Wuhan University, Wuhan, 430071, China

HIGHLIGHTS

- CtCas12a is a thermostable protein with relaxed PAM (YYV). It has been used for pathogen detection and genome editing.

GRAPHICAL ABSTRACT

Detection and gene editing with CtCas12a.

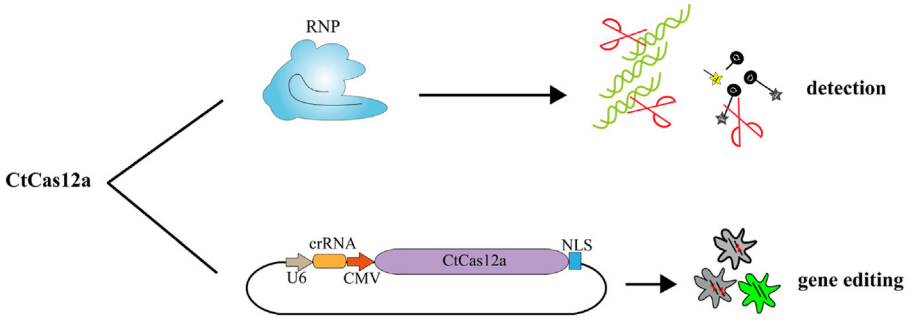

ABSTRACT

CRISPR-Cas12a has been used for genome editing and molecular diagnosis. The well-studied Cas12a orthologs have a T-rich PAM and are usually categorized as non-thermally stable enzymes. Here, we identified a new Cas12a ortholog from *Clostridium thermobutyricum*, which survives at 60 °C. This Cas12a ortholog is named as CtCas12a and exhibits low sequence similarity to the known Cas12a family members. CtCas12a is active in a wide temperature range from 17 to 77 °C. Moreover, this ortholog has a relaxed PAM of YYV (Y=C or T, V = A or C or G). We optimized the conditions for *trans*-cleavage and enabled its detection of nucleic acids. CtCas12a executed genome editing in human cells and generated up to 26% indel formation in the EGFP locus. With the ability to be active at high temperatures as well as having a relaxed PAM sequence, CtCas12a holds potential to be further engineered for pathogen detection and editing a wide range of genomic sequences.

1. Introduction

Archaea and bacteria developed adaptive immunity systems to avoid invasion of foreign nucleic acids (Jinek et al., 2012; Mali et al., 2013; Pickar-Oliver & Gersbach, 2019). One of these adaptive immunity systems, CRISPR-Cas (clustered regularly interspaced short palindromic

* Corresponding author. Department of Clinical Laboratory, Frontier Science Center for Immunology and Metabolism, Medical Research Institute, Zhongnan Hospital of Wuhan University, Wuhan University, Wuhan, 430071, China.
E-mail address: haoyin@whu.edu.cn (H. Yin).

https://doi.org/10.1016/j.cellin.2023.100126
Received 8 September 2023; Received in revised form 8 October 2023; Accepted 8 October 2023
Available online 11 October 2023

repeats and CRISPR-associated proteins), has been discovered and categorized into two classes, class 1 and class 2, based on the amount of effector proteins (Jinek et al., 2012; Mali et al., 2013; Pickar-Oliver & Gersbach, 2019). Class 1 contains multi-unit effector complexes, whereas class 2 functions through a single effector protein (Mohanraju et al., 2016). These classes can be further divided into six CRISPR-Cas types and at least 29 subtypes (Jinek et al., 2012; Mali et al., 2013; Pickar-Oliver & Gersbach, 2019).

Among the identified CRISPR systems, class 2 type II Cas9 system, especially *Streptococcus pyogenes* Cas9 (SpCas9), is widely used in genome editing due to its precision and ease of reprogramming (Jinek et al., 2012; Qiu, Ji, & Zhang, 2022; Yang et al., 2022; Mali et al., 2013; Ran et al., 2013). Under the guidance of CRISPR RNA (crRNA) and *trans*-activating CRISPR RNA (tracrRNA), SpCas9 acts on double-stranded DNA (dsDNA) containing NGG protospacer adjacent motif (PAM) sequence through its two nuclease domains, RuvC and HNH, and produces blunt-ended double-strand break (Jinek et al., 2012; Mali et al., 2013; Ran et al., 2013). The bacterial genomes were analyzed to identify CRISPR sequences using bioinformatics tools, and a number of type V Cas12a proteins were biochemically characterized (Zetsche et al., 2015). These enzymes cleave dsDNA through a single RuvC-like nuclease domain under the guidance of crRNA without tracrRNA, and several Cas12a have been applied to edit the genome of mammalian cells (Fonfara, Richter, Bratovič, Le Rhun, & Charpentier, 2016; Zetsche et al., 2015). In addition, Cas12a holds activities of *trans*-cleavage of single-stranded DNA (ssDNA) after acting on dsDNA, allowing it usage in molecular diagnosis in combination with isothermal amplification technology such as recombinase polymerase amplification (RPA) or loop-mediated isothermal amplification (LAMP) (J. S. Chen et al., 2018; Ding et al., 2020; Gootenberg et al., 2017; Joung et al., 2020; Lu et al.,

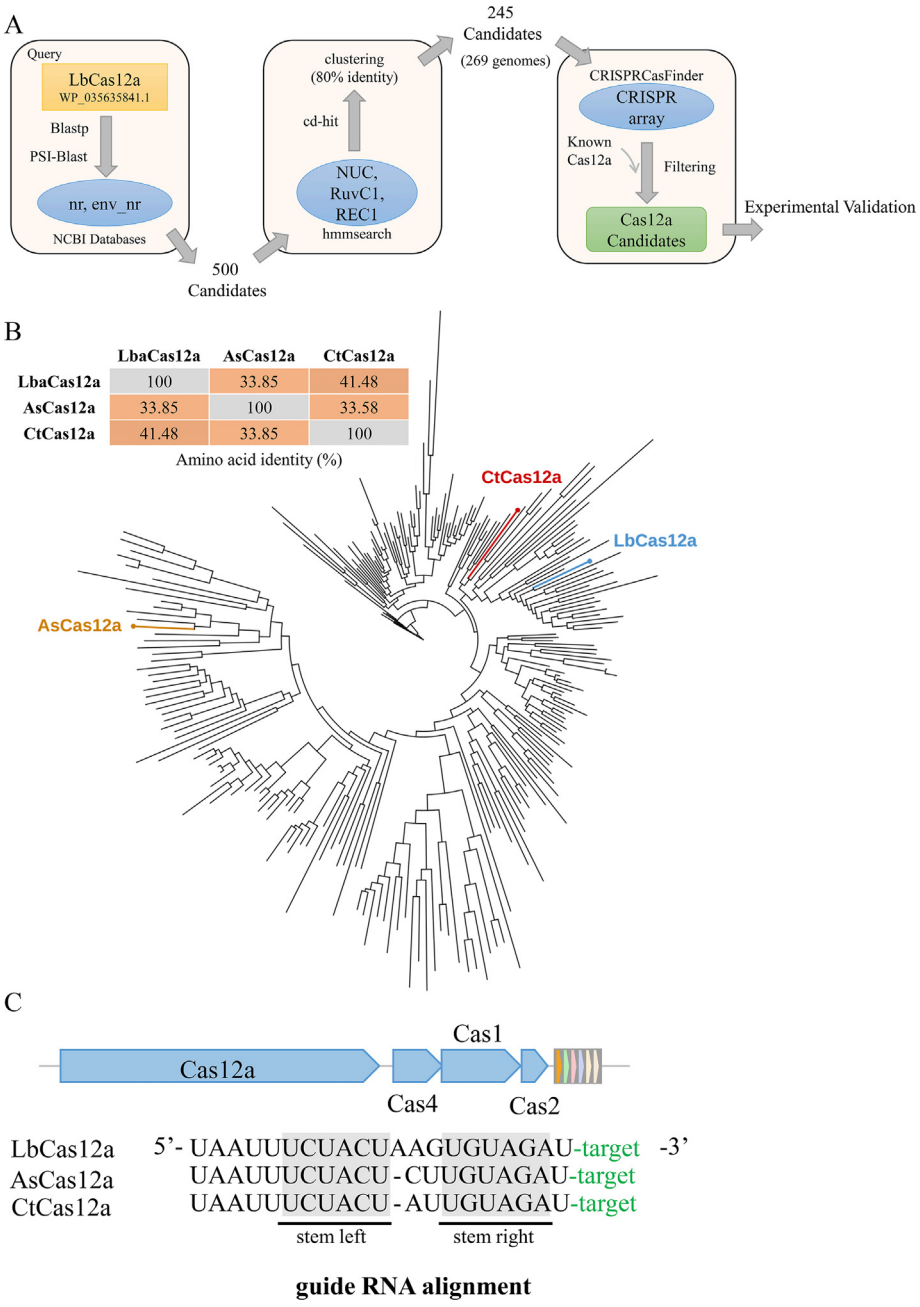

Fig. 1. Identification of CtCas12a and homology comparison. (A) Schematic of diagram for identification of CtCas12a. Candidates were screened out based on blast with LbCas12a as the query. Following domain checking, clustering, and array checking, candidates with low identity to known Cas12a were selected for experimental validation. **(B)** Phylogenetic tree of 245 Cas12a protein sequences. The LbCas12a, AsCas12a, and CtCas12a on the branches of the tree are marked with blue, brown, and red respectively. The percentage of their shared amino acid sequence is shown in the table in (B). **(C)** Loci architecture for CtCas12a and corresponding CRISPR array (top). The crRNA alignment of LbCas12a, AsCas12a, and CtCas12a (bottom). The conserved stem structure is highlighted in grey.

2020; Lu et al., 2022; Teng et al., 2019; H. X. Zhang et al., 2023). However, owing to the restriction of PAM and reaction temperature, the usage of Cas12a is limited. Therefore, it is important to identify new Cas12a members with relaxed PAMs and a wide range of working temperature.

In this study, we discovered and characterized a new Cas12a ortholog. *Clostridium thermobutyricum* Cas12a (CtCas12a) possesses less than 50% sequence similarity to the known Cas12a family members. We identified its PAM preference, cleavage pattern, and the range of working temperature. Furthermore, we optimized the reaction conditions for both *cis*-and *trans*-cleavage, and applied it for nucleic acid detection. With integration of a nuclear localization signal (NLS) and codon optimization, CtCas12a was able to perform genome editing in human cells.

2. Results

2.1. Identification of CtCas12a

To identify more functional Cas12a endonucleases in nature, we developed a computational pipeline illustrated in Fig. 1A. We chose classic *Lachnospiraceae bacterium* ND2006 Cas12a (LbCas12a) as the query to screen the protein from the nr and env_nr database of NCBI by online blastp and PSI-blast tools. Then we clustered candidates containing three complete key domains (NUC, RuvC1, REC1) at 80% identity to narrow down the 245 candidates. After examining the existence of a typical CRISPR array near the candidate using CRISPRCasFinder, we compared the sequence identity between candidates and known Cas12a (Couvin et al., 2018). Three Cas12a candidates with low identity (less than 50%) to known Cas12a were selected for experimental validation. Our preliminary data shows that the *cis*-cleavage activity of *Clostridium thermobutyricum* (Ct) Cas12a is higher than two other candidates (data not shown). Therefore, we chose CtCas12a for further study. Protein sequence comparison and phylogenetic analysis show CtCas12a is with 41.48% amino acid identity to LbCas12a and 33.58% to *Acidaminococcus* sp. BV3L6 (AsCas12a) (Fig. 1B). Although CtCas12a is distinct from LbCas12a or AsCas12a, the genome of CtCas12a is equipped with classic type V-A CRISPR/Cas system including four Cas genes (cas12a, cas4, cas1 and cas2) and an adjacent CRISPR array with 6 spacers (Fig. 1C). Because Cas12a is guided by crRNA, we predicted the crRNA based on CRISPR direct repeat. crRNA alignment shows crRNA from *Clostridium thermobutyricum* is highly conserved reflected in identical stem structure (Fig. 1C). In addition, *Clostridium thermobutyricum* survived at 40–60 °C as well as at pH 5.5 to 8.0, which may imply that CtCas12a has thermotolerance (Canganella, Kuk, Morgan, & Wiegel, 2002). Thus, we hypothesize that CtCas12a may serve as a new tool for genome editing and nucleic acids detection with thermal stability.

2.2. In vitro characterization of PAM preferences and cleavage site of CtCas12a

To explore the activity of CtCas12a system *in vitro*, we purified CtCas12a protein expressed by prokaryotic expression systems (Fig. S1). To identify the PAM preferences of CtCas12a, a PAM library plasmid containing a target sequence and 8 bp randomized nucleotides were constructed and incubated with CtCas12a RNPs. The cleaved products were purified and prepared for next generation sequencing (Fig. 2A) (Shi et al., 2022). We found that there was a noticeable enrichment of T or C at positions −2 and −3 of the PAM sequence but no preference at positions −5 to −8, regardless of whether incubation occurred for 15 min or under more stringent conditions of 5 min incubation (Fig. 2B and C).

To better understand its PAM preference, we mutated the positions −1 to −4 of PAM sequentially to obtain DNA substrates with thirteen PAM combinations (Fig. 2D), and these substrates were incubated with CtCas12a RNP for 5 min and 15 min (Fig. 2E). For each time point and substrate, we quantified cleavage efficiency and plotted on a heatmap (Fig. 2F). When positions −2 and −3 of PAM are A or G and position −1 is T, the cleavage efficiency is substantially reduced, while the change of position −4 has little effect (Fig. 2D–F), indicating that CtCas12a has a PAM preference for YYV (Y═C or T, V = A or C or G).

To confirm the cleavage site, we gel-recovered the cleavage products for Sanger sequencing (Fig. 2G). Similar to LbCas12a, CtCas12a-mediated cleavage caused sticky ends away from PAM, which took place

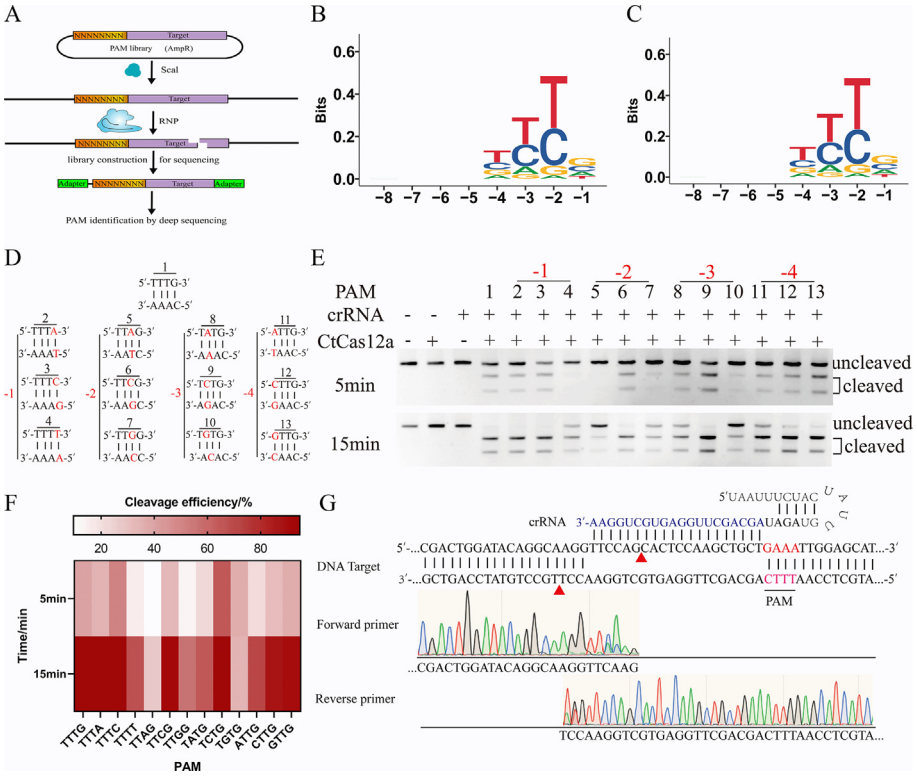

Fig. 2. *In vitro* characterization of PAM preferences and cleavage site of CtCas12a. (A) Schematic of *in vitro* PAM identification of CtCas12a. The PAM library was cleaved by CtCas12a RNPs, followed by the library preparation for sequencing. **(B–C)** Sequence logos obtained by incubating PAM library with CtCas12a RNP at 50 °C for 5 min (B) or 15 min (C). **(D-E)** *In vitro* cleavage of PAM mutant dsDNA substrates by CtCas12a RNP. The mutated sites are positions −1 to −4 of PAM and are marked in red. **(F)** Heatmaps of cleavage efficiency of each PAMs in (D) and (E). **(G)** Sanger sequencing of *in vitro* cleavage products shows that CtCas12a can produce sticky ends. Red triangles indicate cleavage sites.

following the 14th base on the non-targeted strand and the 23rd base on the targeted strand (Zetsche et al., 2015). Collectively, by PAM library screening and single-base mutated PAM-mediated cleavage assays, we showed that CtCas12a was a crRNA-mediated endonuclease which could produce sticky ends and had a relaxed PAM (YYV).

2.3. Optimization of in vitro cis-cleavage

Since the natural strain of CtCas12a can survive at a wide range of temperatures (40–60 °C), we explored whether temperature changes affect the cleavage activity of CtCas12a system (Fig. 3A–C). By changing the pre-incubation temperature of crRNA and protein, we found that as the pre-incubation temperature increased, from 17 °C to 47 °C, the cleavage efficiency gradually increased and reached the optimal pre-incubation temperature at 37 °C (Fig. 3A–C). However, when the pre-incubation temperature was increased to 57 °C, the CtCas12a system completely lost its cleavage ability (Fig. 3B and C). We speculated that crRNA could not form a stable protein-binding stem loop structure due to the high temperature. At the same time, when the cleavage temperature was increased from 17 °C to 77 °C, the protein still maintained cleavage activity and had higher cleavage activity at 47 °C (Fig. 3B and C).

In addition to temperature, enzyme activity can also be affected by many factors, including pH, divalent ion concentration, and reaction time (Jinek et al., 2012; Shi et al., 2022). Therefore, we explored the activity of CtCas12a under different reaction conditions (Fig. S2). When guided by crRNA, CtCas12a cleaved double-stranded DNA in the presence of Mg^{2+} (10 mM) and at a wide range of pH from 6 to -10, with optimal activity at pH 9 (Figs. S2A–C). CtCas12a exhibited a fast cleavage rate for double-stranded DNA, and more than 90% of the cleaved products could be produced within 2 min (Fig. S2D).

To explore the effect of crRNA structure on CtCas12a protein activity, we truncated spacer and scaffold respectively and found that CtCas12a maintained high cleavage activity when spacer length was 18–30 nt and scaffold length was 18–20 nt (Figs. S3A–B). In addition, by mutating and modifying the stem loop structure in crRNA, we found that truncation of the loop region rather than single-base mutation reduced the *cis*-cleavage activity of CtCas12a (Fig. S3C).

2.4. Optimization of the conditions for trans-cleavage activity of CtCas12a

We next investigated the preference of *trans*-cleavage activity of CtCas12a. We used fluorophore quencher (FQ)-labeled single-stranded (ss) DNA as the substrate of *trans*-cleavage (Fig. 4A) (J. S. Chen et al., 2018; Gootenberg et al., 2018; Gootenberg et al., 2017). Four ssDNA containing five bases of poly-A, poly-T, poly-C, or poly-G were chemically synthesized, and each of them was examined as the substrate. CtCas12a could not cleave the poly-G ssDNA to produce any detectable fluorescent signals, while the signals produced using poly-C was much higher than poly-A and poly-T, indicating a "C" preference for *trans*-cleavage of CtCas12a (Fig. 4B). The pH of buffer has been shown to play a role in modulate the *trans*-cleavage activity of Cas12a (Lv et al., 2021). We applied buffer 16 for optimization *cis*-cleavage as previously described with pH number varied from 4 to 10, and identified the pH 9 or 10 showed optimal fluorescence kinetics curve (Fig. 4C) (Shi et al., 2022). To identify an optimal concentration of Mg^{2+} for *trans*-cleavage, we investigated buffer 16 with 0–20 mM Mg^{2+}, and the results indicates that 10 mM Mg^{2+} was sufficient to promote *trans*-cleavage of CtCas12a (Fig. 4D). Taking together, we would use poly-C ssDNA for substrate of *trans*-cleavage, with pH 9 buffer containing 10 mM Mg^{2+} for optimized nucleic acids detection.

2.5. Measurement of the specificity of CtCas12a

To determine the specificity of CtCas12a, we mutated the spacer region to introduce single- or double-nucleotide mismatch, and measure the *cis*- and *trans*-cleavage activities using each mutated crRNA (Fig. 5A–F). Single-nucleotide substitution at the proximal end of the PAM sequence (position 1–6) led to a decrease of *cis*-cleavage activity, while such mutation at the distal end had minimal impact except for the mutation at position 15 (Fig. 5A and B). Consistently, double-nucleotide

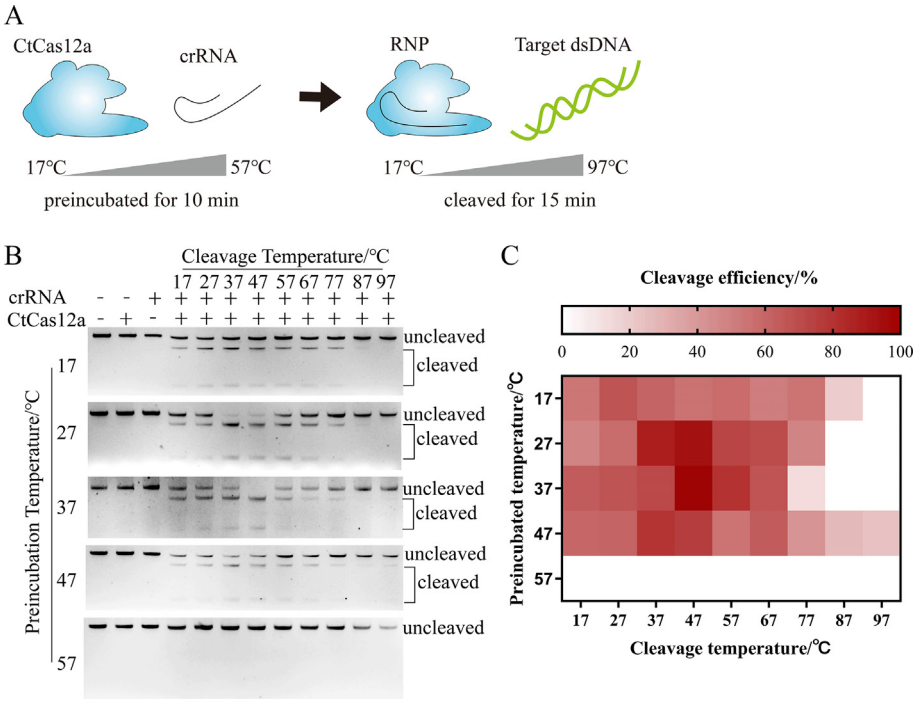

Fig. 3. Effects of pre-incubation and cleavage temperature on CtCas12a activity. (A) Schematic diagram of pre-incubation and cleavage of CtCas12a at gradient temperatures. **(B)** *In vitro cis*-cleavage of double-stranded DNA by CtCas12a under various pre-incubation and cleavage temperatures. **(C)** Heatmap of cleavage efficiency of each temperature in (B).

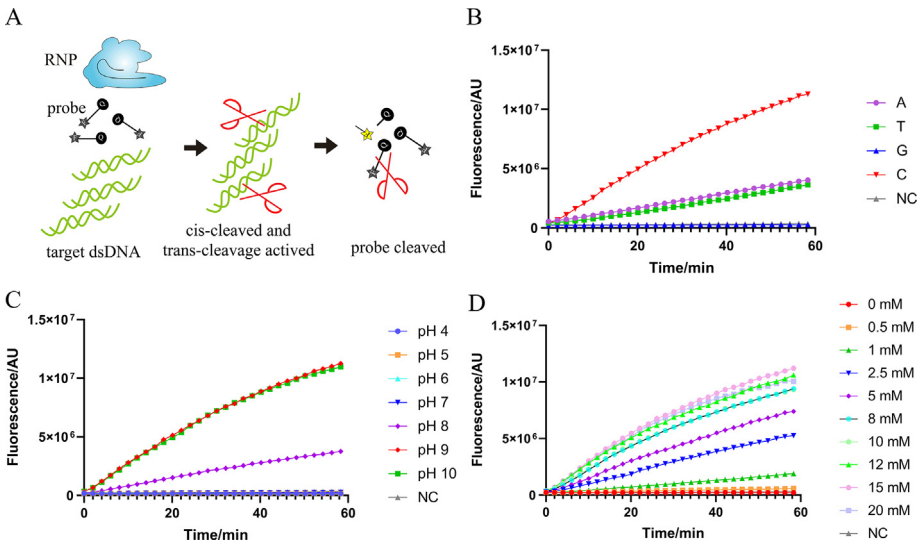

Fig. 4. Optimization of conditions for *trans*-cleavage. (A) Schematic diagram of assay for determining *trans*-cleavage activities. **(B)** Kinetics curve of *trans*-cleavage activities mediated by CtCas12a with ssDNA probe sequence of poly-A, poly-T, poly-C, and poly-G. **(C)** Kinetics curve of *trans*-cleavage activities mediated by CtCas12a in buffer 16 with different pH numbers. **(D)** Kinetics curve of *trans*-cleavage activities mediated by CtCas12a in buffer 16 with different concentrations of Mg^{2+}.

substitutions in positions 1–6, 14/15, 15/16 but not mutations in other positions substantially mitigate *cis*-cleavage activity (Fig. 5D and E). To determine *trans*-cleavage activity, fluorescent values were measured at various time points. Double-nucleotide substitutions showed more profound but not diminished reduction than single-base substitution for *trans*-cleavage for most positions, suggesting that CtCas12a could tolerate point mutations in target sequences for pathogen detection (Fig. 5A–F).

2.6. Nucleic acids detection using CtCas12a

Enterovirus 71 (EV71) is one of the less common viruses to cause hand, foot, and mouth disease (HFMD) among children (Puenpa, Wanlapakorn, Vongpunsawad, & Poovorawan, 2019; Tang et al., 2022; W. Zhang, Huang, Huang, & Zeng, 2020). However, it is the major cause of life-threatening complications of HFMD (Li & Lao, 2017; Sabanathan et al., 2014). Timely diagnosis of EV71 in patients with HFMD symptom can be used to mitigate disease outcomes. A fast and convenient CRISPR-based diagnostics could be suitable for such purpose. Here we applied CtCas12a to detect EV71, in order to explore its potential for pathogen detection.

Two-steps and one-pot CRISPR-based diagnostics have been developed. The substrates were first isothermal amplification, and then the amplified products were transferred for CRISPR detection in two-steps approach; whereas in one-pot reaction the isothermal amplification and CRISPR detection were combined in one tube (Fig. 6A-B)(J. S. Chen et al., 2018; Ding et al., 2020; Gootenberg et al., 2018; Joung et al., 2020; Lu et al., 2020; Lu et al., 2022; Teng et al., 2019; H. X. Zhang et al., 2023). The detection limit for two-steps reaction using CtCas12a reached 200 ag per reaction for DNA substrate containing EV71 sequence, equivalent to ~6.5 copies/uL (Fig. 6C). In contrast, the detection limit for one-pot reaction using CtCas12a was between 2 and 20 fg DNA substrate per reaction (Fig. 6D). These data suggest that the one-pot reaction can be further optimized for CtCas12a-mediated nucleic acids detection.

2.7. Applying CtCas12a for genome editing of human cells

We optimized the codon of CtCas12a for its expression in mammalian cells and integrated a NLS at its C-terminal. We designed crRNAs of CtCas12a against EGFP, and transfected each of them to HEK293T cells stably expressing EGFP (HEK293T-EGFP) (Fig. 7A) (J. Wang et al., 2022). The numbers of EGFP negative cells suggest the efficiencies of genome editing. We examined spacers ranged from 18 to 30 nt in lengths, and the results suggested that 20 nt spacer showed optimal editing efficiency (Fig. 7B). Up to ~40% GFP negative cells was obtained in more than one crRNA used (Fig. 7C). Amplicon sequencing confirmed up to 26% indel formation after CtCas12a treatment using different crRNAs, and deletion of DNA fragment is the major editing outcome (Fig. 7D, S4). The efficiency obtained from amplicon sequencing is lower than the number of GFP negative cells. This discrepancy is likely due to the disruption of transcription by CtCas12a binding to EGFP sequence in a portion of cells. Optimization of plasmid dose further increase GFP negative cells to ~60%, suggesting CtCas12a holds potential for efficient genome editing (Fig. S5).

3. Discussion

In this study, we discovered a new Cas12a protein applying bioinformation tools. CtCas12a exhibited relatively low amino acid similarity with known Cas12a proteins but conserved crRNA structure (Fig. 1). Our data indicates CtCas12a has a relaxed PAM of YYV, in combination with its ability of generation indel formation in human cells, may provide a platform for genome editing with broad sequence selection (Figs. 2 and 7). We have used AlphaFold to obtain the preliminary structure information of CtCas12a (Data not shown). Structure-guided engineering of its the PAM interacting (PI) domain and DNA binding domain, as well as eliminating *trans*-cleavage activity could further improve its efficiency and expand its targeting sequences for genome editing(Ma et al., 2022; Walton, Christie, Whittaker, & Kleinstiver, 2020; L. Zhang et al., 2021). Further codon and NLS optimization could also improve its editing efficiency (Liu et al., 2019). We will examine the engineered CtCas12a in various endogenous sites and cell types. Engineered CtCas12a may hold potential to be superior to well-established LbCas12a and AsCas12a, as well as their variants (Huang et al., 2022; B. P. Kleinstiver et al., 2019; Ma et al., 2022). Catalytically impaired CtCas12a linked with specific deaminase may achieve the base transition of C-to-T or A-to-G (F. Chen et al., 2022; Benjamin P. Kleinstiver et al., 2019; X. Wang et al., 2020).

Our data indicate that CtCas12a is a thermostable protein with optimal enzyme activities at ~50 °C, and its activities remains at ~60 °C (Fig. 3). Most characterized Cas12a family member are not categorized as thermostable proteins. While we were working on CtCas12a, a recent study identified two different thermostable Cas12a protein, as CmeCas12a (*Compostmetagenome* Cas12a) and YmeCas12a (*Yellowstone metagenome* Cas12a) (Fuchs et al., 2022). Together, the presence of these

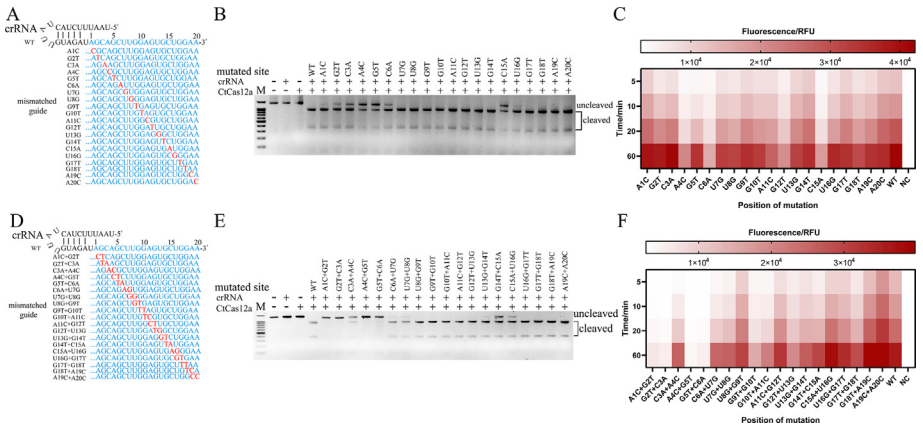

Fig. 5. Tolerance of CtCas12a to mismatch mutations. (A) Illustration of single base-pair mutation in spacer region. **(B)** *Cis*-cleavage of DNA substrates using CtCas12a and single-base pair mutated crRNA for 15 min. **(C)** Heatmap of fluorescent values reflecting *trans*-cleavage activities of CtCas12a with single-base pair mutated crRNA at 5, 10, 20, 60 min. **(D)** Illustration of double base-pair mutation in spacer region. **(E)** *Cis*-cleavage of DNA substrates using CtCas12a and double base-pair mutated crRNA for 15 min. **(F)** Heatmap of fluorescent values reflecting *trans*-cleavage activities of CtCas12a with double base-pair mutated crRNA at 5, 10, 20, 60 min.

Cas12a proteins indicate members of Cas12a could be thermostable.

Thermostable CtCas12a could be combine with LAMP with optimal reaction temperature at ~60 °C (Joung et al., 2020). Through examining various conditions for *trans*-cleavage activities, we obtained optimal conditions for detecting substantial fluorescent signals (Fig. 4). Further studies are warranted to investigate the combination of CtCas12a with LAMP for detection of pathogen. Although CtCas12a could reach high sensitivity of nucleic acids detection in two-steps approaches, its sensitivity for one-pot reactions in combination with RPA is lower (Fig. 6). Further testing is demanded to improve the performance of CtCas12a with isothermal amplification for one-pot detection.

Our data indicates that CtCas12a could tolerate one and two mismatches in non-seed region for both *cis* and *trans*-cleavage *in vitro* (Fig. 5). For application of nucleic acids detection, Cas effector is usually applied after target amplification, and such tolerance would not often cause false positive outcomes due to enrichment of its target sequences by isothermal amplification (J. S. Chen et al., 2018; Ding et al., 2020; Gootenberg et al., 2018; Gootenberg et al., 2017; Joung et al., 2020; Lu et al., 2020; Lu et al., 2022; Teng et al., 2019; H. X. Zhang et al., 2023). In addition, it is worth to explore the potential off-target editing outcomes of CtCas12a in human cells.

In summary, we discovered and characterized a new Cas12a protein with distinct different amino acid sequences. We applied it for detecting nucleic acids and genome editing in human cells. We expected that CtCas12a could be further engineered to be powerful tools for molecular diagnostics and genome editing of human cells.

4. Materials and methods

4.1. Plasmids and oligonucleotides

The DNA fragments for CtCas12a with codon optimization for prokaryotic expression and encoding EV71 VP1 gene were synthesized and cloned into the vectors (GenScript Biotech, Nanjing, China). The substrates used in cleavage assay and detection were obtained by PCR from the synthesized plasmids. After TA cloning (Vazyme), the linear plasmid substrates with PAM single base mutation were prepared by restriction endonuclease ScaI (NEB) digestion. The CtCas12a nuclease mammalian expression plasmid was generated by cloning the mammalian codon optimized CtCas12a sequence (GenScript) into the modified PY016 plasmid (pcDNA3.1-hLbCpf1, Addgene plasmid # 69988). All DNA fragments and oligonucleotides sequences used in this study were listed in the Supplementary Tables 1–5.

4.2. Protein expression and purification

CtCas12a tagged with 6 × His in the C-terminal was cloned into the pET28A vector, a bacterial expression vector (GenScript). *E.coli* BL21 (DE3) containing CtCas12a protein constructs were grown in Terrific Broth at 37 °C. Until the cell density reached 0.6-0.8 OD600, isopropyl β-D-1-thiogalactopyranoside (IPTG, Sangon Biotech) was added for CtCas12a protein induction at 18 °C for 16–18 h. Cells were harvested and resuspended in 20 mM Tris-HCl, pH 7.4, 500 mM NaCl. Then the cells were lysed by sonication (Scientz). After centrifuged at 10,000×*g* for 1 h, the clear supernatant of lysate was collected and filtered with filters (0.22 μm). Supernatant was bound in batch to HisTrap HP (GE Healthcare) and eluted in buffer (20 mM Tris-HCl, pH7.4, 500 mM NaCl) with a gradient of imidazole. Eluted fractions were observed by SDS-PAGE, and protein were collected in expected size. Eluted protein was concentrated to 500 μL by centrifugal filters (Millipore), and quantified by BCA Protein Assay Kit (ThermoFisher Scientific). Finally, the protein was frozen in 20 mM Tris-HCl, pH 7.4, 200 mM NaCl, 50% (v/v) glycerol at −80 °C for future use.

4.3. Synthesis of crRNAs

The DNA templates were provided by overlap extension PCR with forward primers carrying T7 promoter sequence (Tsingke biotechnology). The T7 transcription reaction was performed for 2 h at 37 °C, and then the DNA templates were digested by DNase I (Promega) at 37 °C for 15 min. The crRNAs were purified by the Monarch RNA purification kit (NEB). Primes for production of crRNAs used are listed in Supplementary Tables 2–4.

4.4. Discovery of PAM sequence

Random plasmid library was cloned into pUC19 vector (GenScript) using the spacer and randomized PAM sequence of 8 nucleotides. The linear library was obtained by ScaI (NEB) digestion. The linear library (10 nM) was digested by 100 nM CtCas12a-crRNA (RNP) complex for 5 or 15 min at 50 °C in 20 mM HEPES, pH 9.0, 10 mM KCl, 10 mM $MgCl_2$, 0.1 mM EDTA, 0.5 mM DTT with 20 μL final volume. The reactions were terminated by 1 μL proteinase K (Thermo Fisher) at 55 °C for 10 min. The cleaved products were purified, ligated with adapters (Vazyme) and amplificated with 2 rounds of PCR, with a total of no more than 25 cycles, to build a second-generation sequencing library for NovaSeq. Sequencing reads were filtered by an average Phred quality (Q score) at least 25 and analyzed by Python script. Raw data were standardized according to the control sample, cleaved by the restriction enzyme EcoR I. The seqlogo results were draw by R as previously described (Wagih, 2017).

4.5. In vitro cleavage assay

Unless otherwise indicated, preincubation was performed with purified CtCas12a protein (50 nM) and crRNA (50 nM) in 20 mM HEPES, pH9.0, 10 mM $MgCl_2$, 10 mM KCl, 0.5 mM DTT, 0.1 mM EDTA for 10 min

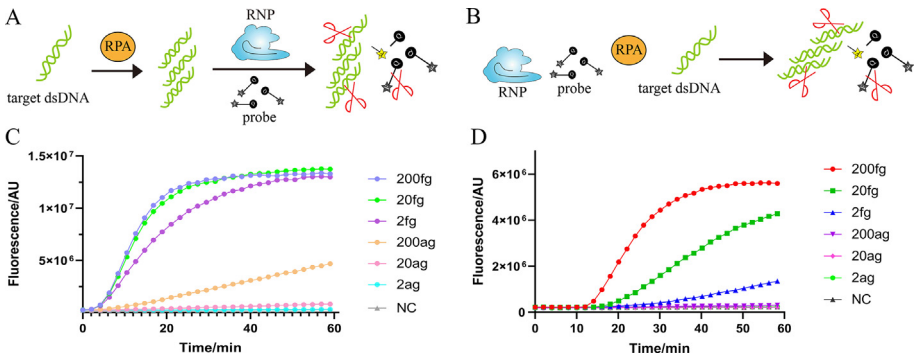

Fig. 6. Nucleic acids detection using CtCas12a. (A-B) Schematic diagram of CtCas12 for nucleic acids detection using two-steps approach (A) or one-pot reaction **(B)**. **(C-D)** Detection limit of CtCas12a for DNA encoding EV71 VP1 gene sequences using two-steps approach **(C)** or one-pot reaction **(D)**.

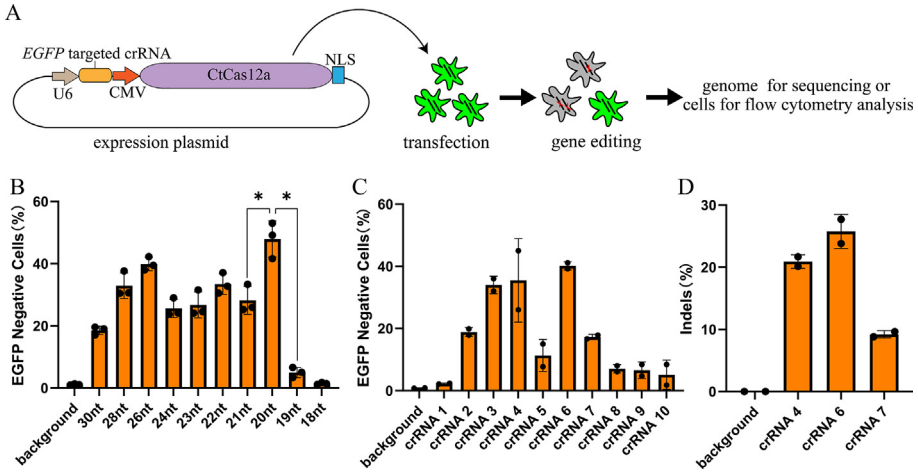

Fig. 7. Genome editing by CtCas12a in human cells. (A) Schematic diagram of assay for genome editing in HEK293T-EGFP cells. **(B)** Flow cytometry analysis of EGFP disruption using crRNA with varied lengths of spacer. **(C)** Flow cytometry analysis of EGFP disruption using different crRNAs. **(D)** Amplicon sequencing for EGFP disruption using representative crRNAs in **(C)**.

at 37 °C to form the RNP complex. The cleavage reaction (20 μL final volume) was initiated by the addition of 3 nM target DNA (Supplementary Table 1) and incubated at 47 °C for 15 min. The reaction was terminated with addition of proteinase K for 10 min at 55 °C. Cleaved products were run on 2% TAE agarose gel. Image Lab software (Bio-rad) was employed to quantify the cleavage efficiency.

4.6. Fluorescent reporter assay for trans-cleavage activity

RNP was preincubated, and quenched fluorescent DNA reporter was added (Takara biotechnology) (Supplementary Tables 3–4). The reaction was initiated by addition of 10 nM target DNA. proceed at 37 °C or 47 °C in SpectraMax i3x (Molecular Devices, λex: 485 nm; λem: 535 nm), or varied temperature in qPCR machine (Bio-rad) for 1 h with fluorescent kinetics measurement.

4.7. Nucleic acids detection using CtCas12a

Two-steps detection of EV71 DNA was consisted of amplification by RPA (Weifang Amp-Future Biotech, Shandong, China) followed by CtCas12a detection. Briefly, 50 μL reactions containing 1 μL sample, 2 μL forward and reverse primer (10 μM, Supplementary Table 4) respectively, 29.4 μL buffer A, 2.5 μL buffer B, nuclease-free water and RPA mix were incubated at 37 °C for 10 min. For detection, 100 nM CtCas12a,100 nM crRNA, 400 nM quenched fluorescent DNA reporter was added to a 96-well black plate (Corning), and RPA reaction products (3 μL) was transferred to the reaction with 20 μL final volume. Reactions were proceeded in SpectraMax i3x (Molecular Devices, λex: 485 nm; λem: 535 nm) for 1 h at 37 °C with fluorescent kinetics measurement.

One-pot detection assay with 20 μL final volume consisted of DNA substrate, 8 μL RPA mixture without buffer B (Weifang Amp-Future Biotech, Shandong, China), 100 nM CtCas12a, 100 nM crRNA, 400 nM ssDNA-FQ reporter, and 2.5 μL B Buffer in black plate (Corning). The detection was performed as described above.

4.8. Cell culture, GFP detection, and amplicon sequencing

HEK293T and HEK293T-EGFP cells were cultured in DMEM with 1% Penicillin/Streptomycin and 10% FBS in a CO_2 incubator (5%) at 37 °C. HEK293T-EGFP cells were prepared as previously described (J. Wang et al., 2022). Cells were seeded on 24-well plates at 1×10^5 cells. After 14–16 h, 1 μg of CtCas12a and crRNA expression plasmids were transfected at 50% cell density with calcium phosphate. Cells were collected at 3 or 5 days after transfection for amplicon sequencing and flow cytometry (Agilent), respectively. For amplicon sequencing, cells were lysed (Davis et al., 2023). The genome cleavage site of EGFP were amplified with two-round PCR, and barcodes as well as the P5 and P7 adapters were added. Fastp software was used to merge the raw paired-end reads to generate full-length reads (S. Chen, Zhou, Chen, & Gu, 2018). Reads with adaptor contamination or a mean quality score <30 were discarded with Trimmomatic tool (Bolger, Lohse, & Usadel, 2014). Alignment of reads to a reference sequence was performed using CRISPResso2 (Clement et al., 2019).

Data availability

The data that support the findings of current study are available within this manuscript and its supplementary information. The amplicon sequencing are available from the Sequence Read Archive (SRA) of NCBI under accession number PRJNA1013157.

Declaration of competing interest

The authors declare no competing interests.

Acknowledgments

This work is kindly supported by Key R&D Program of Hubei Province (2022BCA089 to H.Y., 2022ACA005 to Y.Z), National Key R&D Program of China (2019YFA0802801, 2018YFA0801401, 2022YFF1002801), National Natural Science Foundation of China (31871345 and 32071442 to H.Y., 31972936 to Y.Z.), Medical Science Advancement Program (Basic Medical Sciences) of Wuhan University (TFJC2018004), the Fundamental Research Funds for the Central Universities (2042022dx0003, 2042022kf1190) and the startup funding from Wuhan University (to H.Y. and Y.Z.). We thank Chuan Gao and the core facility of Medical Research Institute at Wuhan University for their technical supports.

Appendix A. Supplementary data

Supplementary data to this article can be found online at https://doi.org/10.1016/j.cellin.2023.100126.

References

Bolger, A. M., Lohse, M., & Usadel, B. (2014). Trimmomatic: A flexible trimmer for illumina sequence data. *Bioinformatics, 30*(15), 2114–2120. https://doi.org/10.1093/bioinformatics/btu170

Canganella, F., Kuk, S. U., Morgan, H., & Wiegel, J. (2002). Clostridium thermobutyricum: Growth studies and stimulation of butyrate formation by acetate supplementation. *Microbiological Research, 157*(2), 149–156.

Chen, F., Lian, M., Ma, B., Gou, S., Luo, X., Yang, K., … Lai, L. (2022). Multiplexed base editing through Cas12a variant-mediated cytosine and adenine base editors. *Communications Biology, 5*(1), 1163. https://doi.org/10.1038/s42003-022-04152-8

Chen, J. S., Ma, E., Harrington, L. B., Da Costa, M., Tian, X., Palefsky, J. M., et al. (2018). CRISPR-Cas12a target binding unleashes indiscriminate single-stranded DNase activity. *Science, 360*(6387), 436–439. https://doi.org/10.1126/science.aar6245

Chen, S., Zhou, Y., Chen, Y., & Gu, J. (2018). fastp: an ultra-fast all-in-one FASTQ preprocessor. *Bioinformatics, 34*(17), i884–i890. https://doi.org/10.1093/bioinformatics/bty560

Clement, K., Rees, H., Canver, M. C., Gehrke, J. M., Farouni, R., Hsu, J. Y., … Pinello, L. (2019). CRISPResso2 provides accurate and rapid genome editing sequence analysis. *Nature Biotechnology, 37*(3), 224–226. https://doi.org/10.1038/s41587-019-0032-3

Couvin, D., Bernheim, A., Toffano-Nioche, C., Touchon, M., Michalik, J., Néron, B., … Pourcel, C. (2018). CRISPRCasFinder, an update of CRISRFinder, includes a portable version, enhanced performance and integrates search for Cas proteins. *Nucleic Acids Research, 46*(W1), W246–w251. https://doi.org/10.1093/nar/gky425

Davis, J. R., Banskota, S., Levy, J. M., Newby, G. A., Wang, X., Anzalone, A. V., … Liu, D. R. (2023). Efficient prime editing in mouse brain, liver and heart with dual AAVs. *Nature Biotechnology*. https://doi.org/10.1038/s41587-023-01758-z

Ding, X., Yin, K., Li, Z., Lalla, R. V., Ballesteros, E., Sfeir, M. M., et al. (2020). Ultrasensitive and visual detection of SARS-CoV-2 using all-in-one dual CRISPR-Cas12a assay. *Nature Communications, 11*(1), 4711. https://doi.org/10.1038/s41467-020-18575-6

Fonfara, I., Richter, H., Bratovič, M., Le Rhun, A., & Charpentier, E. (2016). The CRISPR-associated DNA-cleaving enzyme Cpf1 also processes precursor CRISPR RNA. *Nature, 532*(7600), 517–521. https://doi.org/10.1038/nature17945

Fuchs, R. T., Curcuru, J. L., Mabuchi, M., Noireterre, A., Weigele, P. R., Sun, Z., et al. (2022). Characterization of cme and yme thermostable Cas12a orthologs. *Communications Biology, 5*(1), 325. https://doi.org/10.1038/s42003-022-03275-2

Gootenberg, J. S., Abudayyeh, O. O., Kellner, M. J., Joung, J., Collins, J. J., & Zhang, F. (2018). Multiplexed and portable nucleic acid detection platform with Cas13, Cas12a, and Csm6. *Science, 360*(6387), 439–444. https://doi.org/10.1126/science.aaq0179

Gootenberg, J. S., Abudayyeh, O. O., Lee, J. W., Essletzbichler, P., Dy, A. J., Joung, J., … Zhang, F. (2017). Nucleic acid detection with CRISPR-Cas13a/C2c2. *Science, 356*(6336), 438–442. https://doi.org/10.1126/science.aam9321

Huang, H., Huang, G., Tan, Z., Hu, Y., Shan, L., Zhou, J., … Rong, Z. (2022). Engineered Cas12a-Plus nuclease enables gene editing with enhanced activity and specificity. *BMC Biology, 20*(1), 91. https://doi.org/10.1186/s12915-022-01296-1

Jinek, M., Chylinski, K., Fonfara, I., Hauer, M., Doudna, J. A., & Charpentier, E. (2012). A programmable dual-RNA-guided DNA endonuclease in adaptive bacterial immunity. *Science, 337*(6096), 816–821. https://doi.org/10.1126/science.1225829

Joung, J., Ladha, A., Saito, M., Kim, N. G., Woolley, A. E., Segel, M., … Zhang, F. (2020). Detection of SARS-CoV-2 with SHERLOCK one-pot testing. *New England Journal of Medicine, 383*(15), 1492–1494. https://doi.org/10.1056/NEJMc2026172

Kleinstiver, B. P., Sousa, A. A., Walton, R. T., Tak, Y. E., Hsu, J. Y., Clement, K., … Joung, J. K. (2019). Engineered CRISPR-Cas12a variants with increased activities and improved targeting ranges for gene, epigenetic and base editing. *Nature Biotechnology, 37*(3), 276–282. https://doi.org/10.1038/s41587-018-0011-0

Li, H. G., & Lao, Q. (2017). The pulmonary complications associated with EV71-infected hand-foot-mouth disease. *Radiology of Infectious Diseases, 4*(4).

Liu, P., Luk, K., Shin, M., Idrizi, F., Kwok, S., Roscoe, B., … Wolfe, S. A. (2019). Enhanced Cas12a editing in mammalian cells and zebrafish. *Nucleic Acids Research, 47*(8), 4169–4180. https://doi.org/10.1093/nar/gkz184

Lu, S., Li, F., Chen, Q., Wu, J., Duan, J., Lei, X., … Yin, H. (2020). Rapid detection of African swine fever virus using Cas12a-based portable paper diagnostics. *Cell Discov, 6*, 18. https://doi.org/10.1038/s41421-020-0151-5

Lu, S., Tong, X., Han, Y., Zhang, K., Zhang, Y., Chen, Q., … Yin, H. (2022). Fast and sensitive detection of SARS-CoV-2 RNA using suboptimal protospacer adjacent motifs for Cas12a. *Nature Biomedical Engineering, 6*(3), 286–297. https://doi.org/10.1038/s41551-022-00861-x

Lv, H., Wang, J., Zhang, J., Chen, Y., Yin, L., Jin, D., … Wang, J. (2021). Definition of CRISPR Cas12a T rans-cleavage units to facilitate CRISPR diagnostics. *Frontiers in Microbiology, 12*, Article 766464. https://doi.org/10.3389/fmicb.2021.766464

Ma, E., Chen, K., Shi, H., Stahl, E. C., Adler, B., Trinidad, M., … Doudna, J. A. (2022). Improved genome editing by an engineered CRISPR-Cas12a. *Nucleic Acids Research, 50*(22), 12689–12701. https://doi.org/10.1093/nar/gkac1192

Mali, P., Yang, L., Esvelt, K. M., Aach, J., Guell, M., DiCarlo, J. E., … Church, G. M. (2013). RNA-guided human genome engineering via Cas9. *Science, 339*(6121), 823–826. https://doi.org/10.1126/science.1232033

Mohanraju, P., Makarova, K. S., Zetsche, B., Zhang, F., Koonin, E. V., & van der Oost, J. (2016). Diverse evolutionary roots and mechanistic variations of the CRISPR-Cas systems. *Science, 353*(6299), Article aad5147. https://doi.org/10.1126/science.aad5147

Pickar-Oliver, A., & Gersbach, C. A. (2019). The next generation of CRISPR-Cas technologies and applications. *Nature Reviews Molecular Cell Biology, 20*(8), 490–507. https://doi.org/10.1038/s41580-019-0131-5

Puenpa, J., Wanlapakorn, N., Vongpunsawad, S., & Poovorawan, Y. (2019). The history of enterovirus A71 outbreaks and molecular epidemiology in the asia-pacific region. *Journal of Biomedical Science, 26*(1), 75. https://doi.org/10.1186/s12929-019-0573-2

Qiu, H.-Y., Ji, R.-J., & Zhang, Y. (2022). Current advances of CRISPR-Cas technology in cell therapy. *Cell Insight, 1*, Article 100067.

Ran, F. A., Hsu, P. D., Wright, J., Agarwala, V., Scott, D. A., & Zhang, F. (2013). Genome engineering using the CRISPR-Cas9 system. *Nature Protocols, 8*(11), 2281–2308. https://doi.org/10.1038/nprot.2013.143

Sabanathan, S., Tan le, V., Thwaites, L., Wills, B., Qui, P. T., & Rogier van Doorn, H. (2014). Enterovirus 71 related severe hand, foot and mouth disease outbreaks in South-East Asia: Current situation and ongoing challenges. *Journal of Epidemiology & Community Health, 68*(6), 500–502. https://doi.org/10.1136/jech-2014-203836

Shi, Y. J., Duan, M., Ding, J. M., Wang, F. Q., Bi, L. L., Zhang, C. X., … Zhang, Y. (2022). DNA topology regulates PAM-Cas9 interaction and DNA unwinding to enable near-PAMless cleavage by thermophilic Cas9. *Molecular Cell, 82*(21), 4160–4175. https://doi.org/10.1016/j.molcel.2022.09.032. e4166.

Tang, Q., Xu, Z., Zhang, F., Cai, Y., Chen, Y., Lu, B., … Wu, S. (2022). Identification of a novel binding inhibitor that blocks the interaction between hSCARB2 and VP1 of enterovirus 71. *Cell Insight, 1*, Article 100016.

Teng, F., Guo, L., Cui, T., Wang, X. G., Xu, K., Gao, Q., … Li, W. (2019). CDetection: CRISPR-Cas12b-based DNA detection with sub-attomolar sensitivity and single-base specificity. *Genome Biology, 20*(1), 132. https://doi.org/10.1186/s13059-019-1742-z

Wagih, O. (2017). ggseqlogo: a versatile R package for drawing sequence logos. *Bioinformatics, 33*(22), 3645–3647. https://doi.org/10.1093/bioinformatics/btx469

Walton, R. T., Christie, K. A., Whittaker, M. N., & Kleinstiver, B. P. (2020). Unconstrained genome targeting with near-PAMless engineered CRISPR-Cas9 variants. *Science, 368*(6488), 290–296. https://doi.org/10.1126/science.aba8853

Wang, X., Ding, C., Yu, W., Wang, Y., He, S., Yang, B., … Chen, J. (2020). Cas12a base editors induce efficient and specific editing with low DNA damage response. *Cell Reports, 31*(9), Article 107723. https://doi.org/10.1016/j.celrep.2020.107723

Wang, J., He, Z., Wang, G., Zhang, R., Duan, J., Gao, P., … Yin, H. (2022). Efficient targeted insertion of large DNA fragments without DNA donors. *Nature Methods, 19*(3), 331–340. https://doi.org/10.1038/s41592-022-01399-1

Yang, L.-Z., Gao, B.-Q., Huang, Y., Wang, Y., Yang, L., & Chen, L.-L. (2022). Multi-color RNA imaging with CRISPR-Cas13b systems in living cells. *Cell Insight, 1*, Article 100044.

Zetsche, B., Gootenberg, J. S., Abudayyeh, O. O., Slaymaker, I. M., Makarova, K. S., Essletzbichler, P., … Regev, A. (2015). Cpf1 is a single RNA-guided endonuclease of a class 2 CRISPR-cas system. *Cell, 163*(3).

Zhang, W., Huang, Z., Huang, M., & Zeng, J. (2020). Predicting severe enterovirus 71-infected hand, foot, and mouth disease: Cytokines and chemokines. *Mediators of Inflammation, 2020*, Article 9273241. https://doi.org/10.1155/2020/9273241

Zhang, H. X., Zhang, C., Lu, S., Tong, X., Zhang, K., Yin, H., et al. (2023). Cas12a-based one-pot SNP detection with high accuracy. *Cell Insights, 2*(2), Article 100080. https://doi.org/10.1016/j.cellin.2023.100080

Zhang, L., Zuris, J. A., Viswanathan, R., Edelstein, J. N., Turk, R., Thommandru, B., … Vakulskas, C. A. (2021). AsCas12a ultra nuclease facilitates the rapid generation of therapeutic cell medicines. *Nature Communications, 12*(1), 3908. https://doi.org/10.1038/s41467-021-24017-8